Detection Optimization for Prompt Gamma Ray Imaging during Boron Neutron Capture Therapy (BNCT): A Monte Carlo simulation study

Moo-Sub Kim, Do-Kun Yoon, and Tae Suk Suh*
Department of Biomedical Engineering and Research Institute of Biomedical Engineering, College of Medicine, Catholic University of Korea, Seoul 505, Korea
**Corresponding author: suhsanta@catholic.ac.kr*

1. Introduction

The purpose of this study was the statistical analysis of the prompt gamma ray peak induced by the boron neutron capture therapy (BNCT) from spectra using Monte Carlo simulation. For the simulation, the information of the sixteen detector materials was used to simulate spectra by the neutron capture reaction.

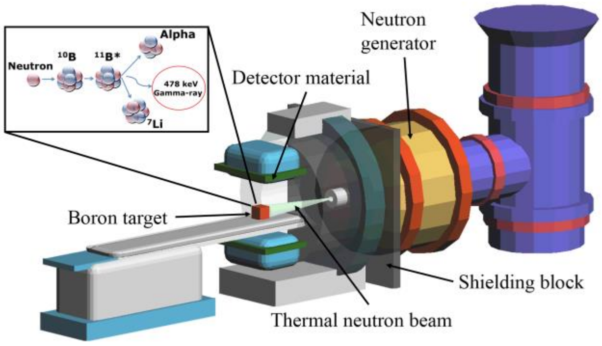

Figure 1. Diagram of simulation of boron neutron capture therapy (BNCT). The information of several detector materials was used to simulate the prompt gamma ray spectra.

2. Methods and Results

The detector size (40.2 cm × 40.2 cm × 8 cm) was fixed to maintain the identical physical factors excluding the materials. [1] The area size of the detector was referred from the specification of actual instruments which is used to the boron neutron capture therapy (BNCT). [1] However, in order to increase the counts number of the gamma ray, the thickness of the detector was set thicker than conventional instruments [2]. The distance between neutron source and the center of target was set at the 100 cm, and the distance between detector and target was defined as the 50 cm. The neutron particle can induce the prompt gamma ray by the nuclear reaction with atoms. Basically, in order to simulate interaction between the material for the gamma ray detection and the photon, the physical and chemical characteristic information of the material for gamma ray detection, such as the density, ratio of the composition atom, and interaction characteristic with the photon, etc., are required. There are two major detector materials (a scintillator and a semiconductor) for the simulation in this study, and the physical and chemical characteristic information of the detector material was inserted to the each simulation. To use Gaussian energy broadening (GEB) function in the MCNPX code, the solutions of the dual equations of full width at half maximum (FWHM) (Eq. (1)) were obtained using the average energy resolution value at the 511 keV and 662 keV, respectively [3].

$$FWHM = a + b\sqrt{E} \qquad (1)$$

a= GEB a (MeV)
b= GEB b ($MeV^{1/2}$)
E= peak energy (MeV)

The solutions 'a' and 'b' were applied to the GEB function in the MCNPX simulation. Because the several simulations about each detector were required to analyze the peaks, the efficient distribution of simulation time was needed. For this reason, the unit of minimum fraction was set as the 10 keV energy bin for the spectrum results by the simulation. The Table 1 shows two GEB values of each detector material, as well as the list of detectors including the density and the average energy resolution values (511 keV and 662 keV) for the simulations. The average energy resolution was acquired by the average calculation using the extracted energy resolution from other research. Thus, the energy resolution values in the Table 1 could not be absolute representative values because of the influence by many factors. After the setting of the GEB values, the prompt gamma ray energy spectra were acquired using the F8 tally. To obtain a more correct energy spectra from the simulations, a boron (density = 2.08 g/cm^3) target was used, and the target size was 10cm^3. In order to induce the active reaction with the target, a thermal neutron (<1eV) source was directed toward the target, and the detectors surrounded the target. The setting of thermal neutron (<1eV) source (4 × 10^7 n/sec) for the MCNPX simulation was referred from the reference research [4].

Table 1. Detector list and specifications (the density, the energy, and the resolution) for the Monte Carlo n-particle extended (MCNPX) simulation. Gaussian energy broadening values (GEB a, GEB b) were calculated using the Eq. (1) with the energy resolution of the 511 and 662 keV.

Detector material	Density (g/cm^3)	Energy resolution 511 keV (%)	Energy resolution 662 keV (%)	GEB a	GEB b
Bismuth Germanate Oxide (BGO)	7.13	14.20	12.50	-0.0050	0.1084
High purity Germanium (HPGe)	5.32	0.70	0.27	0.0164	-0.0180
Cadmium Zinc Telluride (CZT)	5.60	2.00	1.00	0.0360	-0.0360
Lanthanum Chloride (Cerium) ($LaCl_3(Ce)$)	3.64	5.10	3.30	0.0556	-0.0413
Sodium Iodide (Thallium) (NaI(Tl))	3.67	8.60	6.50	0.0486	-0.0065
Cesium Iodide (Thallium) (CsI(Tl))	4.51	9.50	7.70	0.0286	0.0279
Cadmium Telluride (CdTe)	6.20	1.20	2.00	-0.0459	0.0728
Lutetium Yttrium Oxyorthosilicate (LYSO)	7.30	8.00	8.90	-0.0923	0.1864
Gadolinium Oxyorthosilicate (GSO)	6.70	12.00	8.90	0.0760	-0.0205
Lutetium Oxyorthosilicate (LSO)	7.40	10.00	8.40	0.0159	0.0492
Barium Fluoride (BaF_2)	4.90	11.40	8.00	0.0941	-0.0502
Yttrium Aluminum Perovskite (Cerium) (YAP(Ce))	5.40	6.70	5.70	0.0072	0.0378
Lithium Iodide (Eurodium) (LiI(Eu))	4.08	12.90	7.50	0.1814	-0.1615
Bismuth tri-iodide (BiI_3)	5.80	3.80	2.90	0.0201	-0.0010
Mercuric Iodide (HgI_2)	6.40	6.50	5.96	-0.0137	0.0657
Lanthanum Bromide (Cerium) ($LaBr_3(Ce)$)	5.29	4.30	2.80	0.0460	-0.0336

The prompt gamma ray energy spectra induced by the thermal neutrons are shown in Figs. 2(a)-(d).

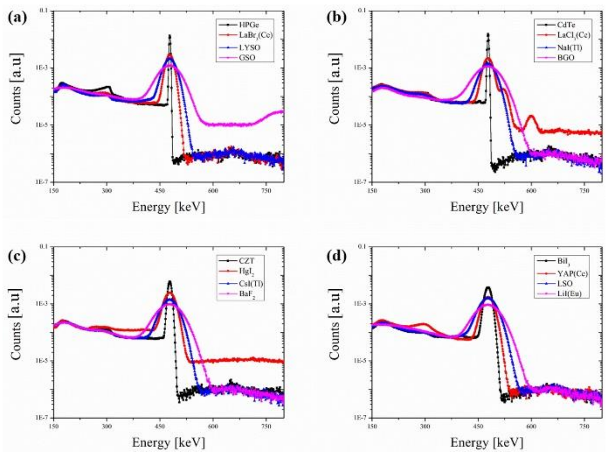

Figure 2. The Monte Carlo n-particle extended (MCNPX) simulations of the sixteen different prompt gamma ray energy spectra. Line colors depending on energy resolution level were assigned to energy spectrum of each detector in the group. (a) HPGe, $LaBr_3$(Ce), LYSO and GSO, (b) CdTe, $LaCl_3$(Ce), NaI(Tl) and BGO, (c) CZT, HgI_2, CsI(Tl) and BaF_2, (d) BiI_3, YAP(Ce), LSO and LiI(Eu) detector materials [5].

In this study, the ten iterative calculations of 478 keV peak were conducted to conclude the energy resolution. The representative value of energy resolution was set using the average value of these ten calculated values.

The method of grouping for the graphs (Figs. 2(a)-(d)) were based on the average value of energy resolution form the table 2. The four detectors of low energy resolution (<3) were assigned as 'good resolution' line to each group. Because only energy resolution was considered to classification of detectors according to their performances, an absolute data of a detector's comprehensive performance cannot be given.

Table 2. Energy resolution values of the 478 keV prompt gamma ray peaks depending on the detector materials. The energy resolution is expressed as a percentage (average values by the ten iterative calculations).

Detector material	Energy resolution at 478 keV (%)
BGO	14.2529
HPGe	0.6279
CZT	2.2989
($LaCl_3$(Ce))	5.4414
NaI(Tl)	9.2315
CsI(Tl)	9.6543
CdTe	0.8367
LYSO	7.517
GSO	12.7999
LSO	10.2113
BaF_2	14.2708
(YAP(Ce))	6.9039
LiI(Eu)	14.5204
BiI_3	3.7672
HgI_2	6.497
($LaBr_3$(Ce))	4.6014

Detection efficiency of 478 keV prompt gamma ray according to the detector material are shown in Fig. 3. Because only detection efficiency was considered to classification of detectors according to their performances, an absolute data of a detector's comprehensive performance cannot be given.

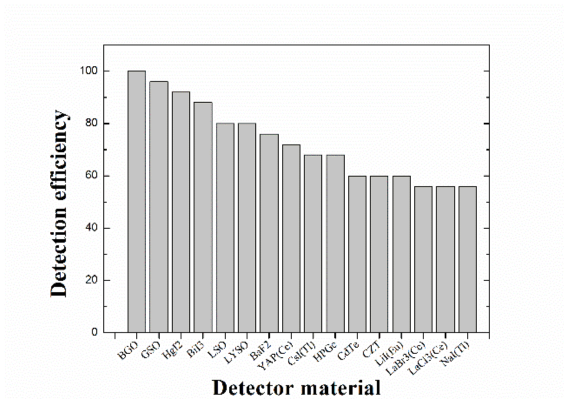

Figure 3. Detection efficiency of 478 keV prompt gamma ray according to the detector material. The standard of normalization was the detection efficiency of BGO. (100%)

3. Conclusions

The results in this study are the first reported data regarding the peak discrimination of 478 keV energy prompt gamma ray using the many cases. (sixteen detector materials). The reliable data based on the Monte Carlo method and statistical method with the identical conditions was deducted. Our results are important data in the BNCT study for the peak detection within actual experiments.

REFERENCES

[1] D.K. Yoon, J.Y. Jung, K.J. Hong, T.S. Suh, Tomographic image of prompt gamma ray from boron neutron capture therapy: A Monte Carlo simulation study, Apl Phys Let, Vol. 104, pp. 083521, 2014.
[2] C. Eleon, B. Perot, C. Carasco, Preliminary Monte Carlo calculations for the UNCOSS neutron–based explosive detector. Nucl Instrum Method Phys Res A, Vol. 619, pp. 234–239 2010.
[3] S. Jakhar, C. Rao, A. Shyam, B. Das, Measurement of 14 MeV neutron flux from DT neutron generator using activation analysis, IEEE Nucl Sci Symp Conf Rec, pp. 2335–2338, 2008.
[4] M. McClish, P. Dokhale, J. Christian, C. Stapels, E. Johnson, F. Augustine, KS. Shah, Performance measurements from LYSO scintillators coupled to a CMOS position sensitive SSPM detector, Nucl Instrum Method Phys Res A, Vol. 652, pp. 264–267 18, 2011.
[5] J. Trummer, E. Auffray, P. Lecoq, A. Petrosyan, P. Sempere-Roldan, Comparison of LuAP and LuYAP crystal properties from statistically significant batches produced with two different growth methods, Nucl Instrum Methods Phys Res A, Vol. 551, pp. 339–351, 2005.